Tumor and Stem Cell Biology

Cancer Research

Genetic Identification of *SEMA3F* as an Antilymphangiogenic Metastasis Suppressor Gene in Head and Neck Squamous Carcinoma

Colleen L. Doçi[1], Constantinos M. Mikelis[1], Michail S. Lionakis[2], Alfredo A. Molinolo[1], and J. Silvio Gutkind[1]

Abstract

Head and neck squamous cell carcinomas (HNSCC) often metastasize to locoregional lymph nodes, and lymph node involvement represents one of the most important prognostic factors of poor clinical outcome. HNSCCs are remarkably lymphangiogenic and represent a clear example of a cancer that utilizes the lymphatic vasculature for malignant dissemination; however, the molecular mechanisms underlying lymphangiogenesis in HNSCC is still poorly understood. Of interest, we found that an axon guidance molecule, *Semaphorin 3F* (*SEMA3F*), is among the top 1% underexpressed genes in HNSCC, and that genomic loss of *SEMA3F* correlates with increased metastasis and decreased survival. SEMA3F acts on its coreceptors, plexins and neuropilins, among which neuropilin-2 (NRP2) is highly expressed in lymphatic endothelial cells (LEC) but not in oral epithelium and most HNSCCs. We show that recombinant SEMA3F promotes LEC collapse and potently inhibits lymphangiogenesis *in vivo*. By reconstituting all possible plexin and neuropilin combinations, we found that SEMA3F acts through multiple receptors, but predominantly requires NRP2 to signal in LECs. Using orthotopic HNSCC metastasis mouse models, we provide direct evidence that *SEMA3F* re-expression diminishes lymphangiogenesis and lymph node metastasis. Furthermore, analysis of a large tissue collection revealed that SEMA3F is progressively lost during HNSCC progression, concomitant with increased tumor lymphangiogenesis. *SEMA3F* is localized to 3p21, an early and frequently deleted locus in HNSCC and many other prevalent human malignancies. Thus, *SEMA3F* may represent an antilymphangiogenic metastasis suppressor gene widely lost during cancer progression, hence serving as a prognostic biomarker and an attractive target for therapeutic intervention to halt metastasis. *Cancer Res; 75(14); 2937–48. ©2015 AACR.*

Introduction

One of the defining hallmarks of cancer is ability to form new vasculature to facilitate the growth and metastatic spread of cancer cells (1). Metastasis is the leading cause of morbidity in patients with a variety of solid tumors, where cancer cells often disseminate through blood and lymphatic vessels (1). Thus, the presence of intra- and peritumoral vasculature is a critical diagnostic and prognostic biomarker (2). Angiogenesis is required for tumors to grow beyond a critical limit and tumor-associated blood vessels have been suggested to participate in metastasis (3). Significantly less is known about the role of lymphangiogenesis in cancer, although lymphatic invasion is one of the most relevant diagnostic parameters for solid tumors (2, 4, 5). Specifically, melanoma and head and neck squamous cell carcinomas (HNSCC)

demonstrate intratumoral lymphangiogenesis that is associated with invasion, metastasis, and decreased survival (6–8). However, the relative contribution of angiogenesis and lymphangiogenesis to cancer progression and metastasis is still not fully understood.

HNSCC is one of the ten most common cancers globally and less than half of patients diagnosed with nonlocalized disease will survive beyond 5 years (9, 10). This is partially attributed to the propensity of HNSCC to metastasize to locoregional lymph nodes, which is the single most significant prognostic indicator and decreases the overall survival rate by more than 50% (11–13). Furthermore, approximately 40% of the lymph nodes in the human body are located within the head and neck region (14), and HNSCC demonstrates significant intratumoral lymphangiogenesis compared with other solid cancers, suggesting that lymphangiogenesis may play a pivotal role in HNSCC metastasis and survival. Therefore, HNSCC may represent a clinically relevant condition to begin to dissect the specific role of lymphangiogenesis in metastasis.

The emergence of deep-sequencing approaches for human disease has led to the identification of a multitude of aberrant molecules in cancer that may contribute to its pathogenesis. While conducting analyses on altered molecules in the HNSCC genome, we observed that *SEMA3F* is among the top 1% underexpressed genes (15). SEMA3F is a member of the class 3 semaphorin family originally characterized in axonal guidance (16). In addition, semaphorins have been shown to play multiple roles in normal and pathologic angiogenesis by acting on their receptors, plexins and neuropilins (17–20). Interestingly, SEMA3F can bind to

[1]Oral and Pharyngeal Cancer Branch, National Institute of Dental and Craniofacial Research, NIH, Bethesda, Maryland. [2]Fungal Pathogenesis Unit, Laboratory of Clinical Infectious Diseases, National Institute of Allergy and Infectious Diseases, NIH, Bethesda, Maryland.

Note: Supplementary data for this article are available at Cancer Research Online (http://cancerres.aacrjournals.org/).

Corresponding Author: J. Silvio Gutkind, Oral and Pharyngeal Cancer Branch, National Institute of Dental and Craniofacial Research, NIH, 30 Convent Drive, Bldg 30, Rm 320, Bethesda, MD 20892. Phone: 301-496-6259; Fax: 301-402-0823; E-mail: sg39v@nih.gov

doi: 10.1158/0008-5472.CAN-14-3121

neuropilin 2 (NRP2), and early studies indicated that SEMA3F expression prevents the growth of metastatic melanoma cells that express high levels of NRP2 (21). However, the relevance of SEMA3F expression in cancers lacking NRP2 has not been investigated. Furthermore, NRP2 is a coreceptor highly expressed on lymphatic endothelial cells (LEC). Therefore, these observations prompted us to explore whether SEMA3F loss may contribute to HNSCC lymphangiogenesis, and hence impact on cancer progression and metastasis.

Materials and Methods

The following represent a brief summary of the procedures. Please see the Supplementary Material for additional detailed methods.

Cell culture

293T-17, HaCat, COS-7, UMSCC2, and UMSCC17B cells were cultured in DMEM + 10% FBS. LECs and HMVECs were cultured in EGM2-MV and human umbilical vein endothelial cells (HUVEC) were cultured in EGM-2 (Lonza). All cells were cultured at 37°C in 5% CO_2. UMSCC2 and UMSCC17B stable cell lines were achieved by selection with 1 μg/mL blasticidin. Transfection of plasmids and siRNAs can be found in the Supplementary Methods. All cell lines underwent DNA authentication (Genetica DNA Laboratories, Inc.) before the described experiments to ensure consistency in cell identity.

The Cancer Genome Atlas analysis

Data regarding the copy number of *PIK3CA* and *SEMA3F* in head and neck cancer was downloaded from the cBio Portal for Cancer Genomics (http://www.cbioportal.org/public-portal/ accessed February 5, 2014).

Immunohistochemistry

Tissue arrays containing normal and oral cancer tissues were purchased from US BioMax Inc. Histopathology of tongue sections was performed as previously described (22). Formalin-fixed paraffin-embedded (FFPE) slides were stained and for tissue arrays were classified on the basis of the intensity and the percentage of positive cells quantified as described (23). Correlations were determined using Pearson coefficient.

SEMA3F purification

Serum-free conditioned medium (CM) from 293T-17 cells expressing NTAP-SEMA3F construct was collected, dialyzed, then isolated using HisTALON cobalt beads (Clontech). ΔFLAG control was generated by incubating purified SEMA3F with anti-FLAG conjugated beads (Sigma-Aldrich) and collecting the unbound supernatant.

Immunoblotting

Cells were lysed in radioimmunoprecipitation assay buffer and concentration was determined using Bio-Rad DC protein assay. Twenty micrograms total protein was separated by SDS-PAGE and transferred to polyvinylidene difluoride membrane overnight at 4°C. Membranes were blocked for 1 hour at room temperature in 5% milk in TBST and then probed with primary antibodies overnight at 4°C. Membranes were washed four times in Tris-buffered saline + 1% Tween-20, probed with horseradish peroxidase–conjugated secondary antibodies for 1 hour at room tem-

perature in 5% milk, washed four times in TBST, and detected using chemiluminescent substrate (Millipore).

Immunofluorescence

For LECs and normal oral keratinocytes (NOK), cells were fixed with 4% paraformaldehyde and permeabilized with 0.1% Triton X-100. LECs were stained with phalloidin-GFP (Invitrogen) and counterstained with Hoescht 33342 (Invitrogen). NOKs were stained with SEMA3F (Sigma-Aldrich) or 58K Golgi Protein (Abcam), imaged with anti-rabbit AlexaFluor 488 (Invitrogen) or anti-goat AlexaFluor 546 (Invitrogen), and counterstained with Hoescht 33342 (Invitrogen). For Matrigel and orthotopic tumor sections, FFPE slides were prepared and stained using the immunohistochemistry protocol described, and then counterstained Hoescht 33342 (Invitrogen). The images were taken using an Axio Imager Z1 microscope equipped with an ApoTome system.

Cell adhesion and collapse assays

For adhesion assays, LEC were treated and plated on collagen-coated plates. Nonadherent cells were removed by washing and adherent cells fixed and stained. For collapse, LECs were transfected with LifeAct GFP and treated, or treated, fixed, and stained with fluorescent phalloidin and nuclear counterstain. Cell area and perimeter were assessed using ImageJ. For heterologous assays, transfected COS-7 cells were treated as indicated. For all assays, quantification was performed using ImageJ from three independent experiments. Statistical significance was determined using one-way ANOVA. For movies, cells were imaged on an Olympus IX-81 inverted confocal microscope with images obtained every 30 seconds for a total of 3 hours, and analyzed using ZEN software (Carl Zeiss).

In vivo lymphangiogenesis assay and FACS

Basement membrane extract (Trevigen) plugs with growth factors and inhibitors, as indicated, were injected subcutaneously into the flank of nude mice. Single-cell suspensions from plugs were prepared as described (24) and cell populations determined by FACS. Statistics were determined using ANOVA from three independent experiments. Cells were resuspended in PBS, stained with a LIVE/DEAD fluorescent dye (L-23105; Invitrogen), and incubated with CD16/32 (2.4G2; BD Biosciences) to block Fc receptors. For staining, cells were incubated with Alexa Fluor 488-conjugated LYVE-1, PE-Cy7-conjugated CD31, allophycocyanin (APC)-conjugated TER-119, APC-Cy7–conjugated CD45 and eFluor 450-conjugated CD102 (eBioscience or BD Biosciences) washed, and analyzed on a 5-laser LSRFortessa (BD Biosciences). Data were analyzed using FACS Diva (BD Biosciences) and FlowJo software (Treestar). Quantification of cell types was performed using PE-conjugated fluorescent counting beads (Spherotech).

Migration assay

Cells were treated as indicated for overnight Boyden migration. Membranes were fixed with methanol, counterstained with hematoxylin, and imaged on an Axiovert microscope. Calculations were based on 18 imaging fields each from three independent experiments. Statistical significance was determined using ANOVA.

Proliferation assay

Cancer cell lines were plated to 60% confluence and transferred to serum-free media with doxycycline for 20 hours. Cells were

incubated an additional 4 hours with 1 μCi [methyl-³H]-thymidine (PerkinElmer). Proliferation was determined by liquid scintillation counting. Statistical significance was determined using ANOVA.

Orthotopic tumor xenografts in SCID/NOD mice

All animal studies were carried out according to NIH-approved protocols (ASP# 10-569), in compliance with the NIH Guide for the Care and Use of Laboratory Animals. Female SCID/NOD mice (NCI) were housed in appropriate sterile filter-capped cages, and fed and watered *ad libitum*. Each animal was injected with 10^5 cells in 50 μL of serum-free media in the tongue. Animals in the control group were fed regular chow, while animals in the prevention group were fed 6 g doxycycline/kg chow 1 week before injection and throughout the study. All animals underwent evaluation of the tongue for disease onset every 3 days, and the observed lesions were assessed for length and width, and tumor volume was determined as described previously (22). Animals were euthanized at the indicated time points and the cervical lymph nodes assessed for evidence of metastases by H&E staining.

Results

SEMA3F expression is lost during HNSCC progression

While analyzing gene expression alterations in HNSCC in available datasets, we observed that *SEMA3F* is among the 1% most downregulated genes [−2.09-fold decrease, $P = 3.6E−20$; ref. 15] and is localized to 3p21, one of the most commonly deleted loci in HNSCC (25). To investigate whether reduced *SEMA3F* expression is caused by genomic alterations, we interrogated the The Cancer Genome Atlas (TCGA) Head and Neck Cancer databases, using *PIK3CA*, one the most frequently amplified genes in HNSCC that is localized to the long arm of the same chromosome (26) as a control (Fig. 1A). Nearly 75% of HNSCC patients showed heterozygous loss of *SEMA3F*, suggesting that this semaphorin may represent a potential tumor suppressor (Fig. 1A). We assessed the Kaplan–Meier univariate survival of patients with heterozygous loss of *SEMA3F* (Fig. 1B) and the Cox proportional hazard multivariate survival, taking into consideration lymph node metastasis (Fig. 1C). In both analyses, *SEMA3F* was a strong negative indicator of survival and a statistically significant independent biomarker [HR = 2.1, $P = 0.01$ and $\exp(\beta) = 1.95$, $P = 0.03$, respectively]. The median survival of patients with heterozygous loss was nearly half of patients expressing normal levels of *SEMA3F* (Fig. 1D). In addition, patients with *SEMA3F* heterozygous loss showed significantly increased percentage of metastatic lymph nodes and lymphovascular invasion (Fig. 1E and F).

SEMA3F loss was reflected at the protein level, as immunohistochemical evaluation of SEMA3F using a SEMA3F-specific antibody (Supplementary Fig. S1) revealed progressive loss of expression with advancing cancer severity. While normal oral epithelium demonstrated high level of SEMA3F expression, this was almost completely abolished in advanced cancers (Fig. 1G). Quantification of a large collection of HNSCC tissues revealed that nearly 70% of the proliferating basal cells in normal oral epithelium expressed high levels of SEMA3F, while over half of HNSCC samples express little to no SEMA3F (Fig. 1H). Interestingly, this correlated with enhanced tumor vascularity, with markers for blood and lymphatic endothelium

significantly increased in the absence of SEMA3F (Fig. 1I and Supplementary Fig. S2). These data support that decreased expression of SEMA3F correlates with poor clinical outcome, increased tumor vascularity, invasion, and metastasis, thus suggesting that SEMA3F may function as a tumor and metastasis suppressor in HNSCC.

SEMA3F is a chemorepulsant for LECs

As the SEMA3F coreceptor NRP2 is highly expressed on LECs (27), we asked whether SEMA3F has a functional impact on these endothelial cells. We engineered a SEMA3F construct that would preserve its extracellular secretion and posttranslational processing while allowing for coexpression of N-terminal tandem affinity purification (NTAP) tags (Fig. 2A). SEMA3F was expressed, fully processed, and the secreted form of the protein was capable of purification using histidine affinity resin (Fig. 2A). Class 3 semaphorins function through a mechanism that involves negative regulation of integrin adhesion to the extracellular matrix, thereby modulating the attachment of endothelial cells to extracellular matrices through cytoskeletal remodeling (28). Secreted SEMA3F was functionally active in HUVEC adhesion assays, and this effect is specific as FLAG-depleted SEMA3F CM but not IgG-depleted CM was no longer able to inhibit attachment (Fig. 2B). Furthermore, SEMA3F caused a dose-dependent decrease of LEC attachment, which was abolished by FLAG-mediated depletion (Fig. 2C). SEMA3F also induced a nearly 80% collapse of the LEC actin cytoskeleton, while decreasing cell perimeter by less than 3% (Fig. 2D). Using either purified SEMA3F or FLAG-depleted control, we documented the cellular collapse using live-cell imaging in LECs expressing fluorescent actin (Supplementary Movies S1 and S2). SEMA3F induced significant retraction of the LEC cytoskeleton, while little change in actin was observed in the FLAG-depleted control (Fig. 2E). Together, this indicates that SEMA3F can be purified in a biologically active form that is capable of negatively regulating the function of LECs.

SEMA3F inhibits LEC function *in vivo*

We next asked whether SEMA3F can function as antilymphangiogenic factor *in vivo*. Matrigel combined with different growth factors were implanted in flanks of nude mice and invaded cells were identified and quantified by FACS. As proangiogenic growth factors such as VEGF-A and -C use neuropilins as coreceptors (16), sphingosine-1-phosphate (S1P), and basic fibroblast growth factor (bFGF) were substituted to circumvent any potential competition with SEMA3F. A stepwise gating strategy was employed to identify specific types of vascular-associated cells and endothelial cells while excluding immune-reactive cells like macrophages (Supplementary Fig. S3). Using Matrigel alone as a negative control and S1P and bFGF as a positive control, we tested the ability of purified SEMA3F to block chemoattractant-mediated endothelial cell recruitment in a dose-dependent, quantitative *in vivo* setting (Fig. 3).

Gross evaluation and H&E-staining Matrigel plugs demonstrated strong infiltration of vasculature in the positive control that was attenuated by SEMA3F addition (Fig. 3A, top and middle). Immunofluorescence against vascular (CD31) and lymphatic (LYVE-1) vessels demonstrate a SEMA3F dose-dependent decrease in S1P- and bFGF-induced vessel recruitment (Fig. 3A, bottom). SEMA3F caused approximately 70% decrease in the abundance of red blood cells, long-regarded as the standard for angiogenesis implantation assays (Fig. 3B; ref. 29). Similarly,
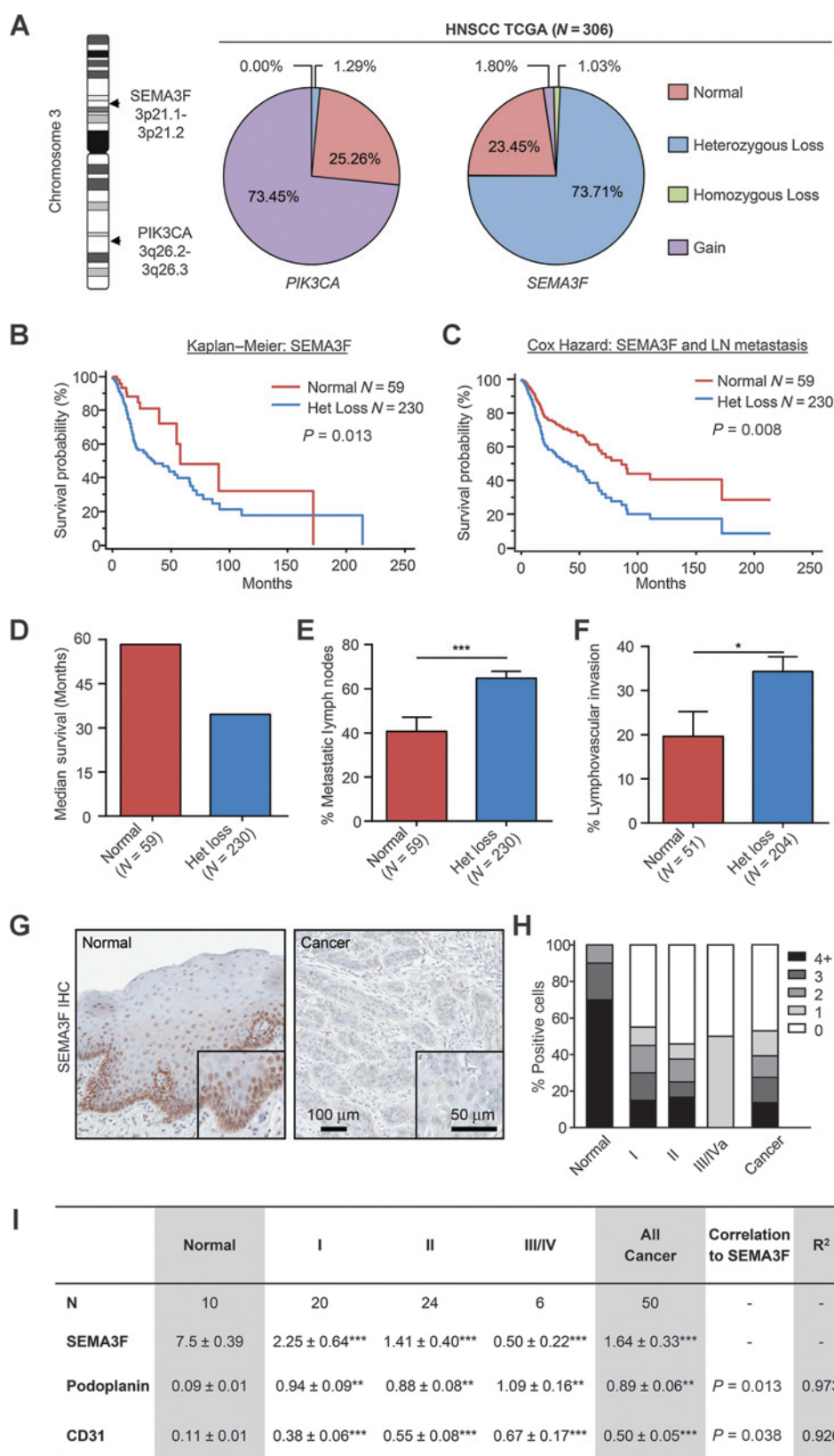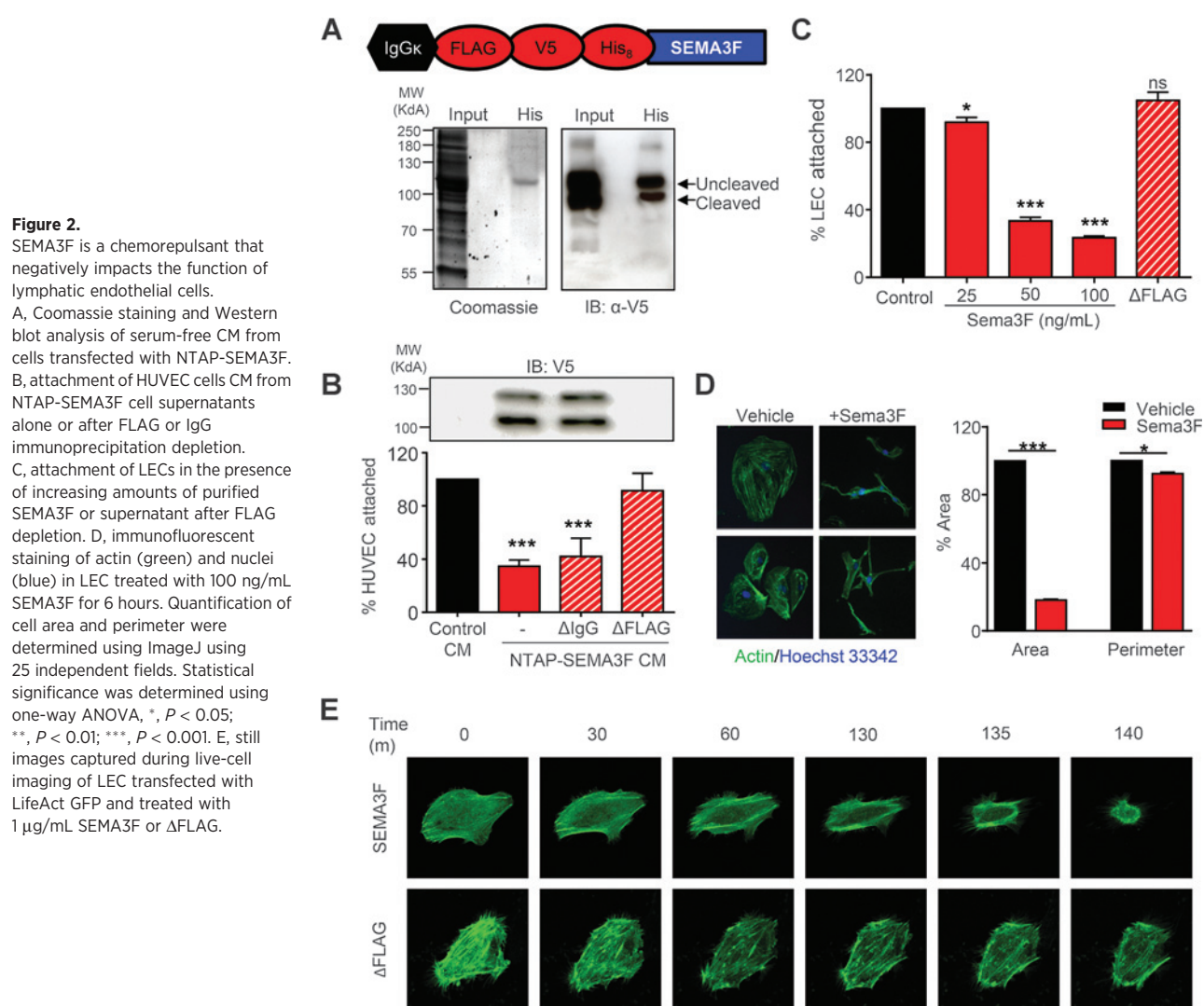
Doçi et al.

Figure 1.
SEMA3F expression is lost during head and neck cancer progression. A, *SEMA3F* (3p21.1–3p21.2) and *PIK3CA* (3q26.2–2q26.3) are located on chromosome 3 and their genomic copy number in head and neck cancer patients according to TCGA was calculated. Clinical outcome for patients with normal (CN = 2) or *SEMA3F* heterozygous loss (CN = 1) were interrogated and Kaplan–Meier (B) and Cox proportional hazard survival curves (C), median survival (D), evidence of metastatic disease (E), and lymphovascular invasion (F) were determined. G, immunohistochemistry of SEMA3F in primary tumor sections of normal oral epithelium and cancer. H, quantification of SEMA3F staining in a tissue array including normal oral epithelium, stage I, II, III, and IV cancers cases. Tissues were evaluated for intensity and percentage of positive cells, with 0 being absent staining and 4+ being intense staining in all cells. I, the same array was also stained for podoplanin (lymphatic vessels) and CD31 (blood vessels), and correlation to SEMA3F expression was calculated using Pearson coefficient. Statistical significance compared to normal was determined by Student t test, **, $P < 0.01$; ***, $P < 0.001$.

	Normal	I	II	III/IV	All Cancer	Correlation to SEMA3F	R²
N	10	20	24	6	50	-	-
SEMA3F	7.5 ± 0.39	2.25 ± 0.64***	1.41 ± 0.40***	0.50 ± 0.22***	1.64 ± 0.33***	-	-
Podoplanin	0.09 ± 0.01	0.94 ± 0.09**	0.88 ± 0.08**	1.09 ± 0.16**	0.89 ± 0.06**	$P = 0.013$	0.973
CD31	0.11 ± 0.01	0.38 ± 0.06***	0.55 ± 0.08***	0.67 ± 0.17***	0.50 ± 0.05***	$P = 0.038$	0.926

Figure 2.
SEMA3F is a chemorepulsant that negatively impacts the function of lymphatic endothelial cells. A, Coomassie staining and Western blot analysis of serum-free CM from cells transfected with NTAP-SEMA3F. B, attachment of HUVEC cells CM from NTAP-SEMA3F cell supernatants alone or after FLAG or IgG immunoprecipitation depletion. C, attachment of LECs in the presence of increasing amounts of purified SEMA3F or supernatant after FLAG depletion. D, immunofluorescent staining of actin (green) and nuclei (blue) in LEC treated with 100 ng/mL SEMA3F for 6 hours. Quantification of cell area and perimeter were determined using ImageJ using 25 independent fields. Statistical significance was determined using one-way ANOVA, *, $P < 0.05$; **, $P < 0.01$; ***, $P < 0.001$. E, still images captured during live-cell imaging of LEC transfected with LifeAct GFP and treated with 1 µg/mL SEMA3F or ΔFLAG.

we saw 60% to 70% decreased abundance of total $CD31^+$ $CD102^+$ endothelial cells (Fig. 3C) and vascular endothelial cells expressing little to no LYVE-1 ($LYVE-1^{low}$), consistent with an antiangiogenic function previously reported for SEMA3F (Fig. 3D; refs. 21, 30, 31). Remarkably, SEMA3F prevented the recruitment of LECs (defined as $LYVE-1^{hi}$), with a 70% to 85% reduction in the abundance of LECs with respect to control plugs (Fig. 3E). Thus, SEMA3F has potent antiangiogenic activity and an even more robust antilymphangiogenic function.

NRP and plexin A coreceptor complexes are sufficient for SEMA3F signaling

NRP2 and plexin A family members are capable of binding to SEMA3F (32, 33), but the relative contribution of each member of this family to SEMA3F-mediated signaling is unknown. Primary HUVEC, human microvascular endothelial cells (HMVEC), and LEC express NRP1, NRP2, and plexin A family members to varying degrees, while COS-7 cells do not express any of these receptors endogenously, thus serving as a heterologous system to investigate SEMA3F signaling (Fig. 4A). Each of the NRP and plexin A family members were expressed in COS-7 cells to test their relative

contribution to SEMA3F signaling alone and in coreceptor complexes (Fig. 4B). As a control, we also tested the effect of SEMA3A, as this semaphorin signals primarily through NRP1-Plexin A1 and NRP1-Plexin A3 (34).

Neither NRPs nor plexins alone were sufficient for SEMA3F or SEMA3A signaling (Fig. 4C and D). SEMA3A was most effective in cells expressing NRP1 and plexin A1, as predicted. SEMA3F potently induced the collapse of COS-7 cells that expressed NRP2 and plexin A3, although cells expressing NRP2 and plexin A1 also collapsed when compared with controls. Interestingly, a modest collapse was observed in SEMA3F-treated cells that expressed NRP1 and plexin A3, and to a lesser degree in those that expressed NRP1 and plexin A1. Some broader effect of SEMA3A was also observed, as NRP2-Plexin A1 complexes and NRP1-Plexin A4 complexes showed collapse. Plexin D1, a receptor for SEMA3E, did not appear to play a role in SEMA3F function (Supplementary Fig. S4). On the basis of these results, we summarized the relative contribution of different receptor combinations to SEMA3F-induced cytoskeletal collapse (Fig. 4E). Finally, we performed live cell imaging of the collapse in COS-7 cells transfected with NRP2 control or NRP2 and plexin A3 treated with SEMA3F

Doçi et al.
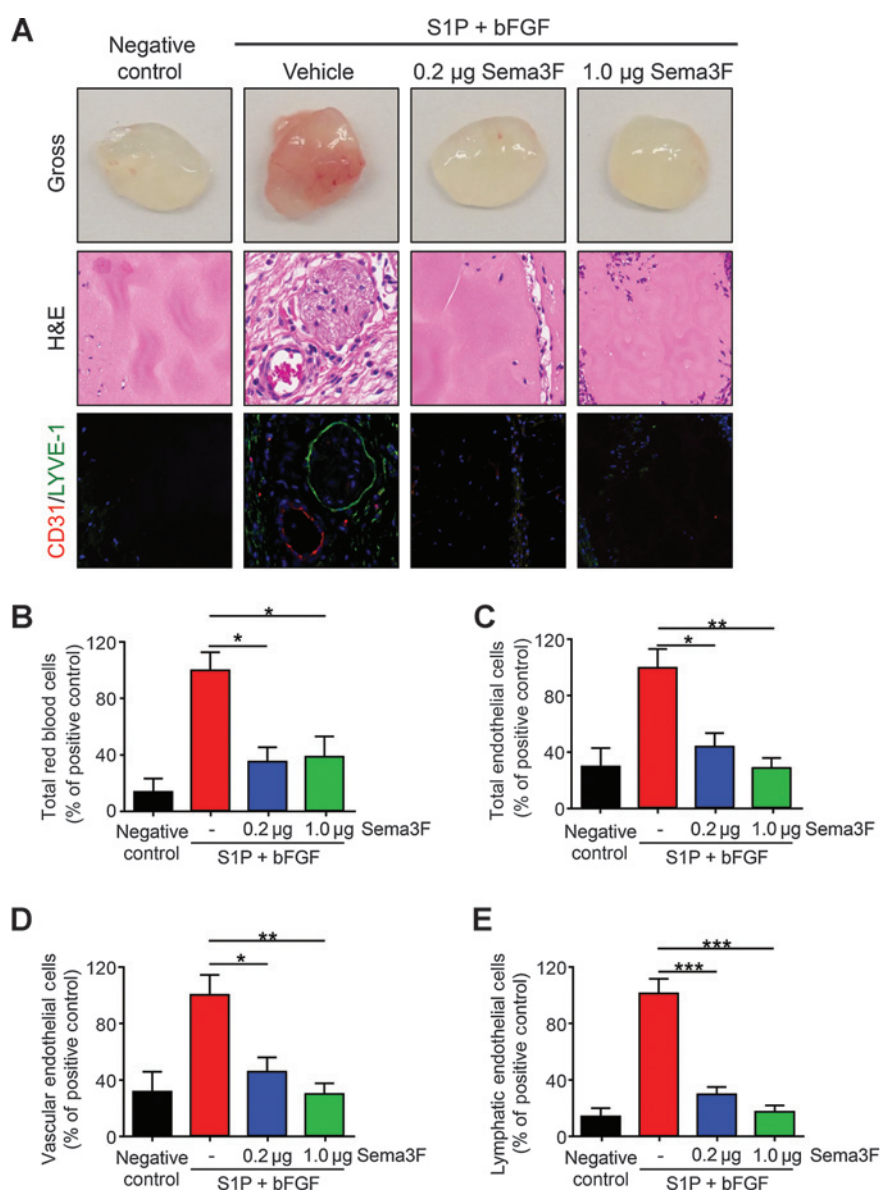
Figure 3.
SEMA3F inhibits *in vivo* lymphangiogenesis. A, Matrigel plugs containing the indicated factors were examined for gross histology (top row), H&E (middle row), and immunofluorescence for CD31 (red) and LYVE1 (green; bottom row). FACS analysis of the number of total red blood cells (B), total $CD102^+CD31^+$ endothelial cells (C), LYVE-1^{low} vascular endothelial cells (D), and LYVE-1^{hi} lymphatic endothelial cells (E) are shown. Values were expressed as a percentage of the stimulated vehicle control from three independent experiments. Statistical significance was determined using one-way ANOVA, *, $P < 0.05$; **, $P < 0.01$; ***, $P < 0.001$.

(Supplementary Movies S3–S4). Control cells demonstrated no changes in the actin cytoskeleton, while expression of NRP2 and plexin A3 was sufficient to induce a rapid collapse phenotype with significant alterations in the actin cytoskeleton (Fig. 4F).

NRP2 is predominantly required for SEMA3F signaling

To determine whether both endogenous NRP1 and NRP2 are necessary for SEMA3F signaling, we abolished expression of these receptors using siRNAs in LECs. Little to no NRP expression remained in siRNA-targeted cells, with no apparent cross-specificity between the knockdown sequences (Fig. 5A). Loss of NRP1 expression only modestly attenuated the collapse of the cells upon SEMA3F treatment; however, significantly less collapse was observed in SEMA3F-treated LEC that do not express NRP2 (Fig. 5B). In a dose–response collapse (Fig. 5C) and attachment (Fig. 5D) assay, loss of NRP1 slightly inhibited the effectiveness of low doses of SEMA3F. In both assays, however, NRP2 knockdown had a pronounced effect, suggesting that NRP2 is the dominant

SEMA3F receptor in LECs. This was further documented by log-dose response analysis (Fig. 5E). While loss of NRP1 increased the IC_{50} of SEMA3F slightly compared with control, NRP2-deficient cells required nearly ten times more SEMA3F to achieve the same effect. Taken together, these findings suggest that while NRP1 may play a role in transmitting SEMA3F signal in the absence of NRP2, NRP2 is predominately required for SEMA3F biologic responses in LECs.

A subset of HNSCC cells express NRP2 and respond to the antitumor activity of SEMA3F

NOKs and most HNSCC cancer cells do not express NRP1 or NRP2. However, a subset of HNSCC cell lines acquired expression of NRP2 (Fig. 6A). Aligned with this observation, increased NRP2 mRNA expression correlates with loss of SEMA3F ($P = 0.003$), poor prognosis, and decreased survival (Supplementary Fig. S5). To test the effect of SEMA3F in HNSCC cells with or without NRP2, we chose two representative highly tumorigenic and

Figure 4.
NRP and plexin A coreceptors coordinate SEMA3F function. A, Western blot analysis demonstrating expression of the NRP, plexin, and VEGFR family members in a panel of immortalized and primary epithelial and endothelial cells. B, Western blot analysis demonstrated specific expression of each NRP and plexin A family member in COS-7 cells. C, COS-7 cells stably expressing GFP were transfected and treated as indicated. Collapse was quantified using ImageJ relative to vehicle control based on 25 imaging fields, each from quadruplicate wells in three independent experiments. Statistical significance was determined using one-way ANOVA, *, $P < 0.05$; **, $P < 0.01$; ***, $P < 0.001$. D, representative images of cells transfected with different receptor combinations and treated with vehicle, SEMA3F, or SEMA3A. E, table summarizing the relative contributions of the different receptor combinations tested. F, confocal images of COS-7 cells transfected with LifeAct-GFP, NRP2, and/or plexin A3 and treated with SEMA3F or ΔFLAG. Images were taken 1 and 3 hours after treatment with SEMA3F.
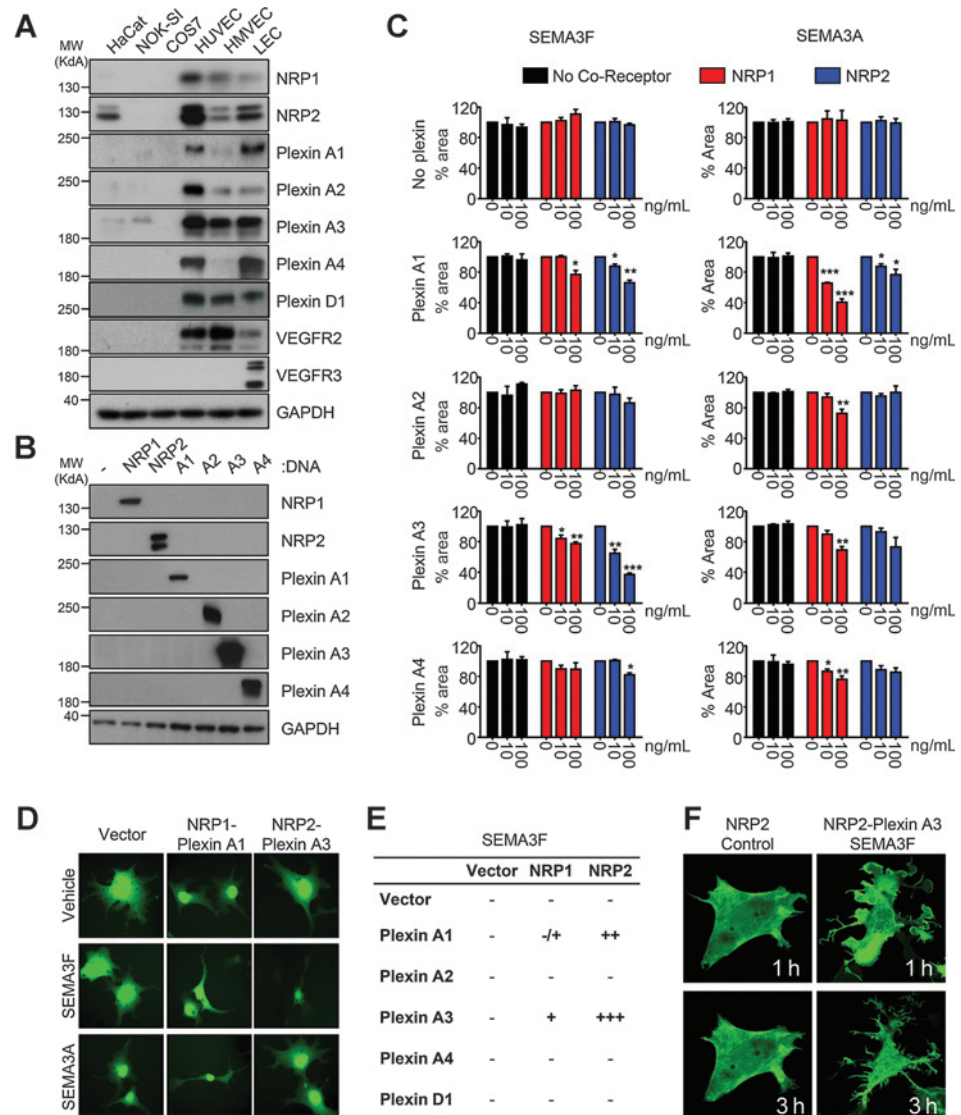
metastatic HNSCC cell lines (22), UMSCC17B, which do not express NRPs, and UMSCC2, with high level expression of NRP2. As an experimental approach, we used a doxycycline-inducible system and confirmed that doxycycline addition induced SEMA3F expression without changing the expression of NRP1 or NRP2 in these cells (Fig. 6B). In both cell types, expression of the rtTA3 tetracycline-dependent transactivating complex alone had no effect on proliferation (Fig. 6C and D). SEMA3F expression inhibited proliferation of UMSCC2 cells significantly; however, this effect was abrogated upon NRP2 knockdown (Fig. 6C). Conversely, in UMSCC17B cells induction of SEMA3F did not alter proliferation (Fig. 6D). As a gain-of-function strategy, transient expression of NRP2 in UMSCC17B rendered them sensitive to the growth inhibitory activity of SEMA3F (Fig. 6D).

Induction of SEMA3F in UMSCC2 cells also blocked endogenous and directed migration (Fig. 6E). Interestingly, siRNA-mediated loss of NRP2 decreased the endogenous migration of these cells compared with control siRNA, although there was no difference between vehicle- and doxycyline-treated groups (Fig. 6E).

Ectopic expression of NRP2 in UMSCC17B cells was sufficient to enhance cell migration over vector control, and induction of SEMA3F did not alter endogenous UMSCC17B migration unless NRP2 was introduced to these cells (Fig. 6F). Taken together, this supports that HNSCC cells expressing NRP2 may exhibit increased migratory capacity, but that loss of SEMA3F may need to precede gain of NRP2 expression.

SEMA3F functions as a potent HNSCC metastasis suppressor

SEMA3F inhibited the biologic activity of LECs and intratumoral lymphangiogenesis is highly prevalent in HNSCC, suggesting that SEMA3F may suppress metastasis *in vivo* through paracrine mechanisms. To test this hypothesis in the context of NRP2 expression or absence, we injected UMSCC2-rtTA3-SEMA3F and UMSCC17B-rtTA3-SEMA3F cells into the tongues of mice and assessed tumor growth, metastasis, and intratumoral vascularity. Consistent with our observations *in vitro*, doxycycline induction of rtTA3 alone had no effect on tumor growth (Supplementary Fig. S6). SEMA3F induction inhibited tumor growth in the UMSCC2-injected animals (Fig. 7A) and this correlated with a

Doçi et al.
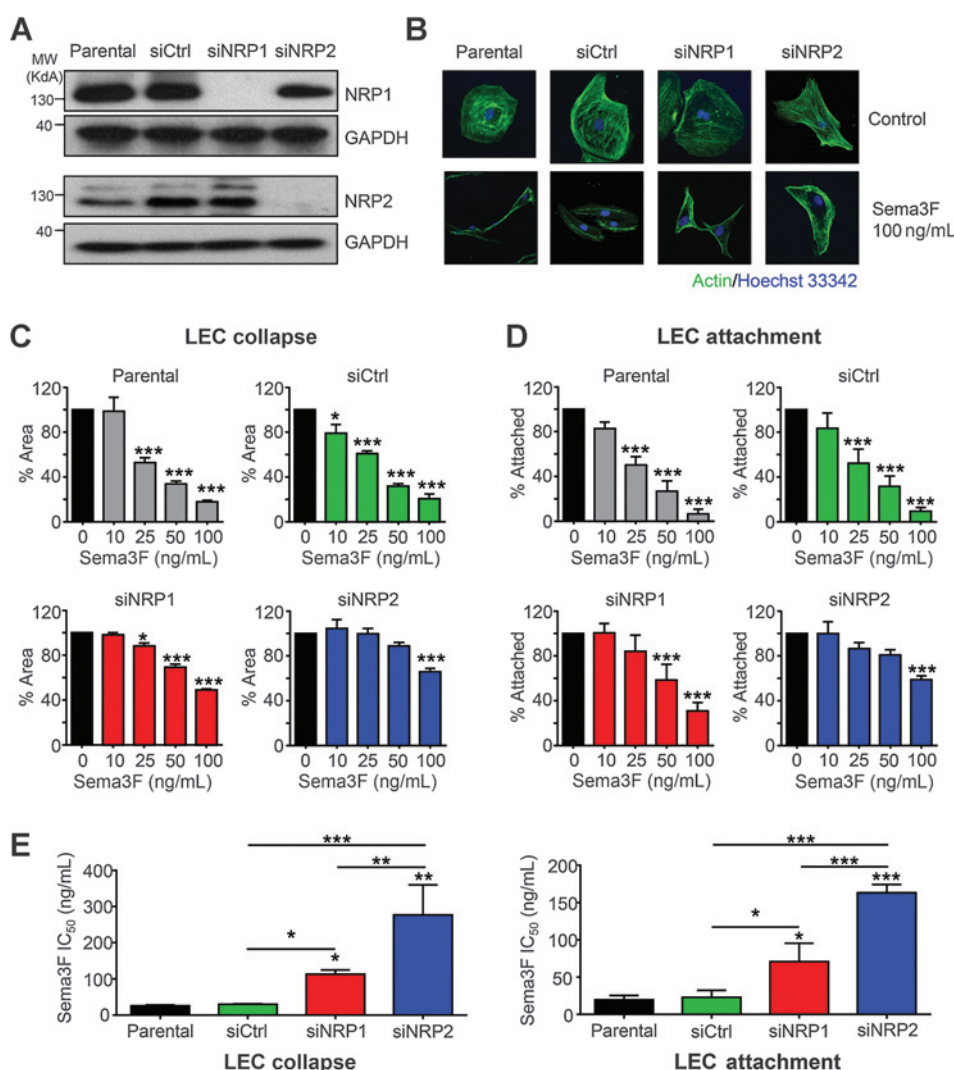
Figure 5.
NRP2 is predominantly required for SEMA3F function in LEC. A, Western blot analysis of endogenous NRP1 and NRP2 in LEC in the presence of control (siCtrl), NRP1, or NRP2 siRNA. B, fluorescent imaging of LEC transfected with the indicated siRNA and then treated with vehicle or 100 ng/mL SEMA3F. Parental and siCtrl-transfected LECs treated with increasing doses of SEMA3F and evaluated for collapse (C) or attachment (D). For both collapse and attachment assays, values are reported relative to vehicle control and quantification was done by ImageJ, based on 25 imaging fields, each from quadruplicate wells in three independent experiments. E, IC_{50} of SEMA3F was calculated from the dose curve generated in C and D. Statistical significance was determined using one-way ANOVA, *, $P < 0.05$; **, $P < 0.01$; ***, $P < 0.001$.

statistically significant decrease in cervical lymph node metastasis (Fig. 7C). Interestingly, SEMA3F induction in UMSCC17B tumors, which do not express NRP2, had no effect on tumor size (Fig. 7B). However, a similar decrease in lymph node metastasis was observed (Fig. 7D). This suggested that the paracrine signaling of SEMA3F to the tumor stroma may be sufficient for suppression of metastasis, while exerting an additional autoinhibitory effect on tumor growth in HNSCC cells that acquired expression of NRP2.

Tongue sections were evaluated by immunohistochemistry for CD31 and LYVE1 and the intratumoral microvessel density (MVD) was quantified. In both the UMSCC2 and UMSCC17B tumors, induction of SEMA3F significantly decreased intratumoral lymphangiogenesis and modestly decreased CD31+ vasculature, albeit not to a statistically significant degree (Fig. 7E and F). As a control, MVD outside the tumor was quantified and was not affected for either CD31 or LYVE1 (Fig. 7E and F). Immunofluorescence staining revealed a high rate of cancer cells infiltrating into lymphatic vessels in control animals that were not observed in SEMA3F-induced cohorts (Fig. 7G and H, white arrows). These results demonstrate that SEMA3F exerts a potent antilymphangiogenic and metastasis suppressor function in HNSCC, and that

SEMA3F may also inhibit growth of a subset of HNSCC expressing NRP2.

Discussion

The tumor microenvironment is regulated through a complex autocrine and paracrine signaling network that is often hijacked and exploited by cancer cells to facilitate their survival, growth, and dissemination. In HNSCC, the interplay of these factors is shifted to promote intratumoral lymphangiogenesis and metastasis, which contribute to poor prognosis and outcome (6, 8). Our findings suggest that SEMA3F is a key antilymphangiogenic molecule that may function at the core of these cell regulatory networks during HNSCC progression. Indeed, loss of SEMA3F is a frequent event in HNSCC, which correlates with increased tumor vascularity and metastasis. We show that SEMA3F can directly affect LEC function *in vitro* and *in vivo* through specific receptor complexes. In COS-7 reconstitution assays, NRP2 and plexin A3 were sufficient to mediate SEMA3F biologic responses, while NRP2-Plexin A1, NRP1-Plexin A3, and NPR1-Plexin A1 complexes can also transduce SEMA3F signals, albeit with decreasing efficiency. NRP2 is the major coreceptor for SEMA3F in LECs,

Figure 6.
NRP2 expression varies in HNSCC and mediates tumor cell responsiveness to SEMA3F. A, Western blot analysis for the expression of receptors in normal oral keratinocytes (NOKSI) and panel of HNSCC cell lines. B, Western blot analysis showing expression of inducible SEMA3F and knockdown or reintroduction of NRP2 expression in UMSCC2 and UMSCC17B cells, respectively. Proliferation assay of UMSCC2-rtTA3-SEMA3F (C) or UMSCC17B-rtTA3-SEMA3F (D) after SEMA3F induction. Cells were treated with control siRNA or NRP2 siRNA (C) or empty vector or NRP2 (D). Migration assay of UMSCC2-rtTA3-SEMA3F (E) or UMSCC17B-rtTA3-SEMA3F (F) cells with no stimulation (vehicle) or towards 20% FBS. Cells were treated with control siRNA or NRP2 siRNA (E) or empty vector or NRP2 (F). Proliferation and migration were reported as a percentage of control. Statistical significance was determined using one-way ANOVA, $*$, $P < 0.05$; $**$, $P < 0.01$; $***$, $P < 0.001$.
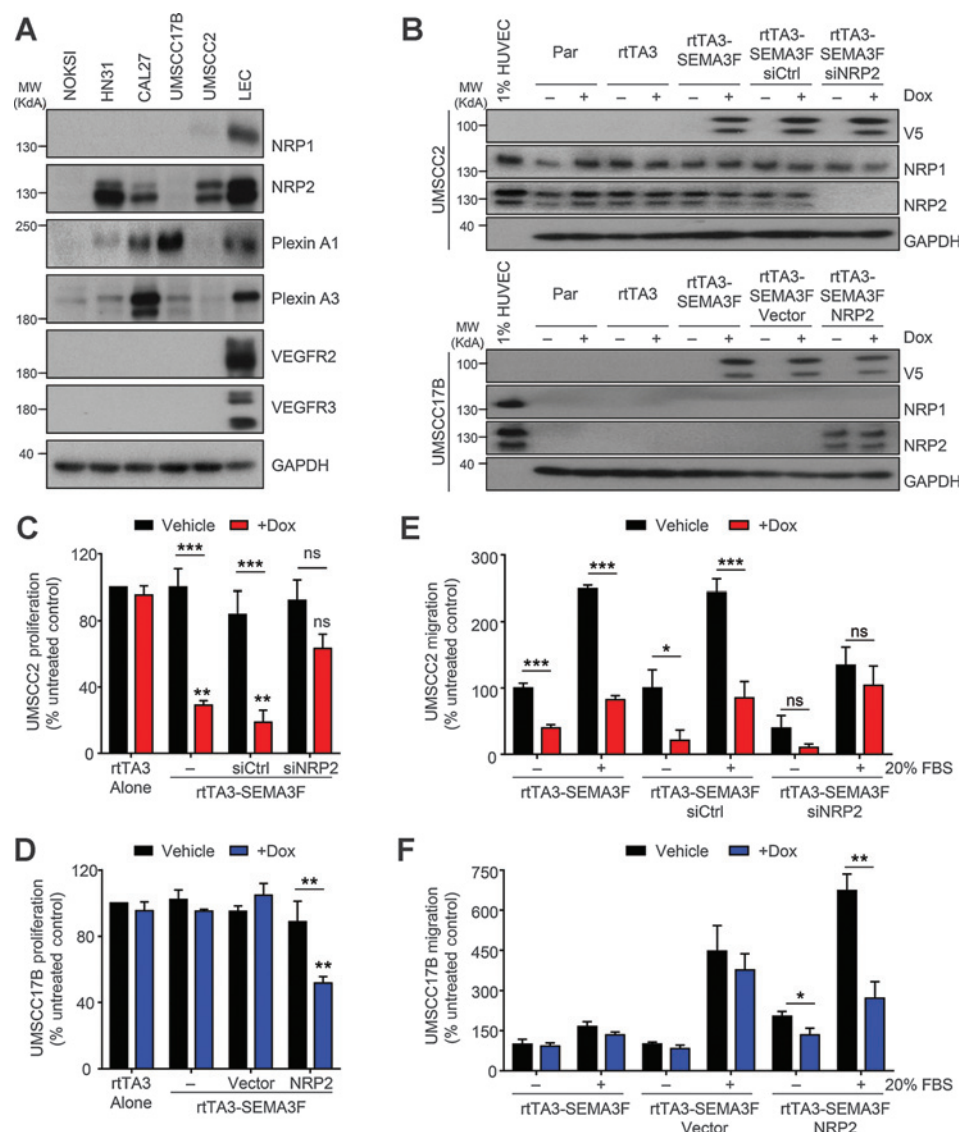
although NRP1 can transmit SEMA3F signals to a lesser extent. Overall, our *in vitro* and *in vivo* studies indicate that SEMA3F is potent antilymphangiogenic molecule. Thus, SEMA3F loss may represent an early event in HNSCC, enabling intratumoral lymphangiogenesis that may contribute to the high prevalence of HNSCC cases presenting with locoregional lymph node invasion, heralding a poor clinical outcome.

NRP2 is a multiligand coreceptor that can both promote and inhibit the development of venous and lymphatic vasculature, in the stroma and on some tumor cells themselves (35–37). In endothelial cells, NRP2 associates with plexin A family members and VEGFR2 and VEGFR3, and these complexes have been implicated in their proangiogenic and -lymphangiogenic signaling (38, 39). Certain malignant epithelial cells express NRP2 without concomitant expression of VEGF receptors (40). The observation that NRP2 but not VEGF receptors are expressed in a subset of HNSCC cells raises the possibility that in these cells NRP2 may act as a coreceptor for plexins or other partners, acting as a gain-of-function alteration during cancer development and progression. Indeed, exogenous NRP2 expression in HNSCC cells enhanced their endogenous migration while loss of upregulated NRP2 in HNSCC cells decreased their endogenous migration. This allows us to hypothesize that cancer cells may be selected for their NRP2 expression due to an increased growth or migratory potential, but that *SEMA3F* loss may need to precede NRP2 gain in HNSCC (Fig. 7I).

Lymphatic metastasis is mainly attributed to increased expression and signaling of proangiogenic factors (2, 5, 41–43). However, expression and secretion of these growth factors alone may not be sufficient for tumor-associated lymphangiogenesis and cancer dissemination. For example, in some cancers VEGF-C or VEGF-D expression levels do not correlate with lymph node metastasis (44, 45), suggesting that other factors may counteract the high level expression of prolymphangiogenic cytokines and attenuate their signaling capacity and prognostic value *in vivo*. On the basis of our current results, one possible explanation is that SEMA3F could repel LECs and thus dominate the activity of VEGF-A and VEGF-C, rendering their expression alone insufficient for

Doçi et al.
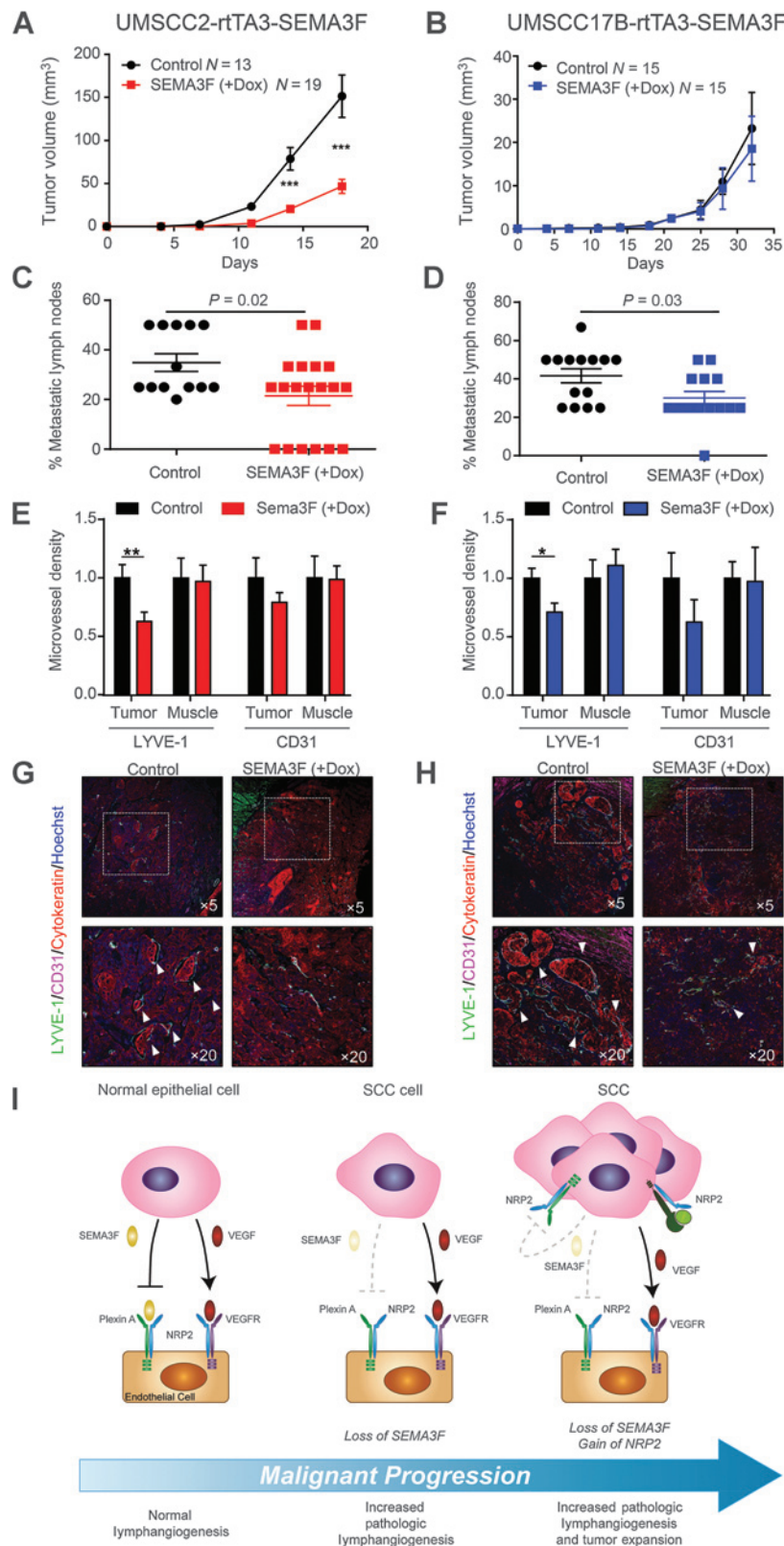
Figure 7.
SEMA3F functions as a tumor and metastasis suppressor *in vivo*. Tumor growth of UMSCC2-rtTA3-SEMA3F (A) and UMSCC17B-rtTA3-SEMA3F (B) after SEMA3F induction via doxycycline chow. Cervical lymph node metastasis was evaluated as the percentage of metastatic lymph nodes in control and doxycycline-fed animals for UMSCC2-rtTA3-SEMA3F (C) and UMSCC17B-rtTA3-SEMA3F (D). MVD for lymphatic (LYVE-1) and blood (CD31) vessels was evaluated in the tumor and muscle of tongues for UMSCC2-rtTA3-SEMA3F (E) and UMSCC17B-rtTA3-SEMA3F (F). MVD was reported relative to the average density in vessels/μm. Statistical significance was determined using Student t test, *, $P < 0.05$; **, $P < 0.01$; ***, $P < 0.001$. Immunofluorescent staining of tumors from control and doxycycline-fed animals for UMSCC2-rtTA3-SEMA3F (G) and UMSCC17B-rtTA3-SEMA3F (H) revealed a higher density and size of vessels in control animals. Lymphovascular invasion by cancer cells is indicated by white arrowheads. I, proposed mechanism for the role of SEMA3F loss in HNSCC. See text for details.

lymphangiogenesis and metastasis. This hypothesis is supported by our findings that induction of SEMA3F alone in orthotopic HNSCC cells significantly inhibits intratumoral lymphangiogenesis and metastasis, even in HNSCC cells that do not express NRP2. Thus, loss of SEMA3F expression in HNSCC may simultaneously enhance VEGF-mediated signaling on endothelial cells and alleviate repressive semaphorin functions, resulting in increased lymphangiogenesis.

Our observation may have a broad impact in multiple highly prevalent human malignancies. In an integrative multiplatform analysis, 3p deletion was identified as a key genomic signature shared by a squamous-like subtype of solid cancers (46). Furthermore, chromosomal loss at 3p21, which is expected to result in the genomic deletion of SEMA3F, has been observed for lung, breast, and kidney cancers in addition to HNSCC (47–50). Immunohistochemistry on HNSCC tumors reveals a complete absence of SEMA3F expression in most advanced cases, suggesting that epigenetic regulation or transcriptional downregulation may contribute to reduced SEMA3F expression of the remaining SEMA3F allele in cancers with SEMA3F heterozygous loss. We can conclude that SEMA3F is a potent chemorepellent molecule for lymphatic and vascular endothelial cells, which acts through NRP2-Plexin A and to a lesser extent NRP1-Plexin A signaling complexes. Loss of SEMA3F is an early event in HNSCC and likely many other highly prevalent human malignancies. This information can in turn be exploited for therapeutic purposes, as most HNSCC lesions may retain one intact SEMA3F allele. This suggests that reactivation of SEMA3F expression or ectopic SEMA3F delivery may offer the opportunity to halt intratumoral lymphangiogenesis and suppress metastasis regardless of the NRP2 expression status of the HNSCC lesion. We can conclude that SEMA3F-NRP2 represents a novel regulatory axis during HNSCC development, progression, and metastasis, thus providing new prognostic markers and therapeutic options in this highly aggressive disease.

Disclosure of Potential Conflicts of Interest

No potential conflicts of interest were disclosed.

Authors' Contributions

Conception and design: C.L. Doçi, J.S. Gutkind
Development of methodology: C.L. Doçi, C.M. Mikelis, A.A. Molinolo, J.S. Gutkind
Acquisition of data (provided animals, acquired and managed patients, provided facilities, etc.): C.L. Doçi, C.M. Mikelis, M.S. Lionakis, A.A. Molinolo
Analysis and interpretation of data (e.g., statistical analysis, biostatistics, computational analysis): C.L. Doçi, M.S. Lionakis, A.A. Molinolo
Writing, review, and/or revision of the manuscript: C.L. Doçi, J.S. Gutkind
Study supervision: J.S. Gutkind

References

1. Hanahan D, Weinberg RA. Hallmarks of cancer: the next generation. Cell 2011;144:646–74.
2. Alitalo K, Tammela T, Petrova TV. Lymphangiogenesis in development and human disease. Nature 2005;438:946–53.
3. Folkman J. Angiogenesis: an organizing principle for drug discovery? Nat Rev Drug Discov 2007;6:273–86.
4. Sundar SS, Ganesan TS. Role of lymphangiogenesis in cancer. J Clin Oncol 2007;25:4298–307.
5. Karaman S, Detmar M. Mechanisms of lymphatic metastasis. J Clin Invest 2014;124:922–8.
6. Beasley NJ, Prevo R, Banerji S, Leek RD, Moore J, van Trappen P, et al. Intratumoral lymphangiogenesis and lymph node metastasis in head and neck cancer. Cancer Res 2002;62:1315–20.
7. Dadras SS, Lange-Asschenfeldt B, Velasco P, Nguyen L, Vora A, Muzikansky A, et al. Tumor lymphangiogenesis predicts melanoma metastasis to sentinel lymph nodes. Mod Pathol 2005;18:1232–42.
8. Kyzas PA, Geleff S, Batistatou A, Agnantis NJ, Stefanou D. Evidence for lymphangiogenesis and its prognostic implications in head and neck squamous cell carcinoma. J Pathol 2005;206:170–7.
9. DeSantis CE, Lin CC, Mariotto AB, Siegel RL, Stein KD, Kramer JL, et al. Cancer treatment and survivorship statistics, 2014. CA Cancer J Clin 2014;64:252–71.
10. Siegel R, Ma J, Zou Z, Jemal A. Cancer statistics, 2014. CA Cancer J Clin 2014;64:9–29.
11. Forastiere A, Koch W, Trotti A, Sidransky D. Head and neck cancer. N Engl J Med 2001;345:1890–900.
12. Leemans CR, Tiwari R, Nauta JJ, van der Waal I, Snow GB. Recurrence at the primary site in head and neck cancer and the significance of neck lymph node metastases as a prognostic factor. Cancer 1994;73:187–90.
13. Shah JP, Candela FC, Poddar AK. The patterns of cervical lymph node metastases from squamous carcinoma of the oral cavity. Cancer 1990;66:109–13.
14. Harisinghani M. Head and neck lymph node anatomy. In:Harisinghani MG, editor. Atlas of lymph node anatomy: Springer, New York; 2013. p 1–29.
15. Rhodes DR, Yu J, Shanker K, Deshpande N, Varambally R, Ghosh D, et al. ONCOMINE: a cancer microarray database and integrated data-mining platform. Neoplasia 2004;6:1–6.
16. Carmeliet P, Tessier-Lavigne M. Common mechanisms of nerve and blood vessel wiring. Nature 2005;436:193–200.
17. Sakurai A, Doci CL, Gutkind JS. Semaphorin signaling in angiogenesis, lymphangiogenesis and cancer. Cell Res 2012;22:23–32.
18. Gaur P, Bielenberg DR, Samuel S, Bose D, Zhou Y, Gray MJ, et al. Role of class 3 semaphorins and their receptors in tumor growth and angiogenesis. Clin Cancer Res 2009;15:6763–70.
19. Neufeld G, Kessler O. The semaphorins: versatile regulators of tumour progression and tumour angiogenesis. Nat Rev Cancer 2008;8:632–45.
20. Tessier-Lavigne M, Goodman CS. The molecular biology of axon guidance. Science 1996;274:1123–33.
21. Bielenberg DR, Hida Y, Shimizu A, Kaipainen A, Kreuter M, Kim CC, et al. Semaphorin 3F, a chemorepulsant for endothelial cells, induces a poorly vascularized, encapsulated, nonmetastatic tumor phenotype. J Clin Invest 2004;114:1260–71.
22. Patel V, Marsh CA, Dorsam RT, Mikelis CM, Masedunskas A, Amornphimoltham P, et al. Decreased lymphangiogenesis and lymph node metastasis by mTOR inhibition in head and neck cancer. Cancer Res 2011;71:7103–12.
23. Amornphimoltham P, Leelahavanichkul K, Molinolo A, Patel V, Gutkind JS. Inhibition of Mammalian target of rapamycin by rapamycin causes the regression of carcinogen-induced skin tumor lesions. Clin Cancer Res 2008;14:8094–101.
24. Nagahashi M, Ramachandran S, Kim EY, Allegood JC, Rashid OM, Yamada A, et al. Sphingosine-1-phosphate produced by sphingosine kinase 1

Doçi et al.

promotes breast cancer progression by stimulating angiogenesis and lymphangiogenesis. Cancer Res 2012;72:726–35.

25. Marescalco MS, Capizzi C, Condorelli DF, Barresi V. Genome-wide analysis of recurrent copy-number alterations and copy-neutral loss of heterozygosity in head and neck squamous cell carcinoma. J Oral Pathol Med 2014;43:20–7.

26. Woenckhaus J, Steger K, Werner E, Fenic I, Gamerdinger U, Dreyer T, et al. Genomic gain of PIK3CA and increased expression of p110alpha are associated with progression of dysplasia into invasive squamous cell carcinoma. J Pathol 2002;198:335–42.

27. Yuan L, Moyon D, Pardanaud L, Breant C, Karkkainen MJ, Alitalo K, et al. Abnormal lymphatic vessel development in neuropilin 2 mutant mice. Development 2002;129:4797–806.

28. Serini G, Valdembri D, Zanivan S, Morterra G, Burkhardt C, Caccavari F, et al. Class 3 semaphorins control vascular morphogenesis by inhibiting integrin function. Nature 2003;424:391–7.

29. Passaniti A, Taylor RM, Pili R, Guo Y, Long PV, Haney JA, et al. A simple, quantitative method for assessing angiogenesis and antiangiogenic agents using reconstituted basement membrane, heparin, and fibroblast growth factor. Lab Invest 1992;67:519–28.

30. Guttmann-Raviv N, Shraga-Heled N, Varshavsky A, Guimaraes-Sternberg C, Kessler O, Neufeld G. Semaphorin-3A and semaphorin-3F work together to repel endothelial cells and to inhibit their survival by induction of apoptosis. J Biol Chem 2007;282:26294–305.

31. Guo HF, Li X, Parker MW, Waltenberger J, Becker PM, Vander Kooi CW. Mechanistic basis for the potent anti-angiogenic activity of semaphorin 3F. Biochemistry 2013;52:7551–8.

32. Xiang X, Zhang X, Huang QL. Plexin A3 is involved in semaphorin 3F-mediated oligodendrocyte precursor cell migration. Neurosci Lett 2012;530:127–32.

33. Giger RJ, Urquhart ER, Gillespie SK, Levengood DV, Ginty DD, Kolodkin AL. Neuropilin-2 is a receptor for semaphorin IV: insight into the structural basis of receptor function and specificity. Neuron 1998;21:1079–92.

34. Takahashi T, Fournier A, Nakamura F, Wang LH, Murakami Y, Kalb RG, et al. Plexin-neuropilin-1 complexes form functional semaphorin-3A receptors. Cell 1999;99:59–69.

35. Klagsbrun M, Eichmann A. A role for axon guidance receptors and ligands in blood vessel development and tumor angiogenesis. Cytokine Growth Factor Rev 2005;16:535–48.

36. Guttmann-Raviv N, Kessler O, Shraga-Heled N, Lange T, Herzog Y, Neufeld G. The neuropilins and their role in tumorigenesis and tumor progression. Cancer Lett 2006;231:1–11.

37. Rizzolio S, Tamagnone L. Multifaceted role of neuropilins in cancer. Curr Med Chem 2011;18:3563–75.

38. Xu Y, Yuan L, Mak J, Pardanaud L, Caunt M, Kasman I, et al. Neuropilin-2 mediates VEGF-C-induced lymphatic sprouting together with VEGFR3. J Cell Biol 2010;188:115–30.

39. Appleton BA, Wu P, Maloney J, Yin J, Liang WC, Stawicki S, et al. Structural studies of neuropilin/antibody complexes provide insights into semaphorin and VEGF binding. EMBO J 2007;26:4902–12.

40. Wild JR, Staton CA, Chapple K, Corfe BM. Neuropilins: expression and roles in the epithelium. Int J Exp Pathol 2012;93:81–103.

41. Mandriota SJ, Jussila L, Jeltsch M, Compagni A, Baetens D, Prevo R, et al. Vascular endothelial growth factor-C-mediated lymphangiogenesis promotes tumour metastasis. EMBO J 2001;20:672–82.

42. Stacker SA, Caesar C, Baldwin ME, Thornton GE, Williams RA, Prevo R, et al. VEGF-D promotes the metastatic spread of tumor cells via the lymphatics. Nat Med 2001;7:186–91.

43. Cao R, Ji H, Feng N, Zhang Y, Yang X, Andersson P, et al. Collaborative interplay between FGF-2 and VEGF-C promotes lymphangiogenesis and metastasis. Proc Natl Acad Sci U S A 2012;109:15894–9.

44. Lahat G, Lazar A, Wang X, Wang WL, Zhu QS, Hunt KK, et al. Increased vascular endothelial growth factor-C expression is insufficient to induce lymphatic metastasis in human soft-tissue sarcomas. Clin Cancer Res 2009;15:2637–46.

45. Ishikawa M, Kitayama J, Kazama S, Nagawa H. Expression of vascular endothelial growth factor C and D (VEGF-C and -D) is an important risk factor for lymphatic metastasis in undifferentiated early gastric carcinoma. Jpn J Clin Oncol 2003;33:21–7.

46. Hoadley KA, Yau C, Wolf DM, Cherniack AD, Tamborero D, Ng S, et al. Multiplatform analysis of 12 cancer types reveals molecular classification within and across tissues of origin. Cell 2014;158: 929–44.

47. Kok K, Naylor SL, Buys CH. Deletions of the short arm of chromosome 3 in solid tumors and the search for suppressor genes. Adv Cancer Res 1997;71:27–92.

48. Sekido Y, Ahmadian M, Wistuba II, Latif F, Bader S, Wei MH, et al. Cloning of a breast cancer homozygous deletion junction narrows the region of search for a 3p21.3 tumor suppressor gene. Oncogene 1998;16:3151–7.

49. Roche J, Boldog F, Robinson M, Robinson L, Varella-Garcia M, Swanton M, et al. Distinct 3p21.3 deletions in lung cancer and identification of a new human semaphorin. Oncogene 1996;12:1289–97.

50. Hesson LB, Cooper WN, Latif F. Evaluation of the 3p21.3 tumour-suppressor gene cluster. Oncogene 2007;26:7283–301.

Cancer Research

AACR American Association for Cancer Research

Genetic Identification of *SEMA3F* as an Antilymphangiogenic Metastasis Suppressor Gene in Head and Neck Squamous Carcinoma

Colleen L. Doçi, Constantinos M. Mikelis, Michail S. Lionakis, et al.

Updated version	Access the most recent version of this article at: doi:10.1158/0008-5472.CAN-14-3121
Supplementary Material	Access the most recent supplemental material at: http://cancerres.aacrjournals.org/content/suppl/2015/05/07/0008-5472.CAN-14-3121.DC1

Cited articles	This article cites 49 articles, 13 of which you can access for free at: http://cancerres.aacrjournals.org/content/75/14/2937.full#ref-list-1
Citing articles	This article has been cited by 4 HighWire-hosted articles. Access the articles at: http://cancerres.aacrjournals.org/content/75/14/2937.full#related-urls

E-mail alerts	Sign up to receive free email-alerts related to this article or journal.
Reprints and Subscriptions	To order reprints of this article or to subscribe to the journal, contact the AACR Publications Department at pubs@aacr.org.
Permissions	To request permission to re-use all or part of this article, use this link http://cancerres.aacrjournals.org/content/75/14/2937. Click on "Request Permissions" which will take you to the Copyright Clearance Center's (CCC) Rightslink site.